

1 *Supplement of*  
2 **Chemical de-staining and the delta correction for blue intensity**  
3 **measurements of stained lake subfossil trees**  
4

5 Feng Wang<sup>1, 2\*</sup>, Dominique Arseneault<sup>1, 2</sup>, Étienne Boucher<sup>3</sup>, Shulong Yu<sup>4</sup>, Steeven Ouellet<sup>1</sup>,  
6 Gwenaëlle Chaillou<sup>5</sup>, Ann Delwaide<sup>6</sup>, Lily Wang<sup>7</sup>

7  
8 <sup>1</sup>Département de Biologie, Chimie et Géographie, Université du Québec à Rimouski, Rimouski, G5L 3A1, Canada

9 <sup>2</sup>Centre d'études nordiques, Université du Québec à Rimouski, Rimouski, G5L 3A1, Canada

10 <sup>3</sup>Département de Géographie, GEOTOP and Centre d'études nordiques, Université du Québec à Montréal,  
11 Montréal, H3A 0B9, Canada

12 <sup>4</sup>Key Laboratory of Tree-ring Physical and Chemical Research and Xinjiang Laboratory of Tree-ring Ecology,  
13 Institute of Desert Meteorology, China Meteorological Administration, Urumqi, 830002, China

14 <sup>5</sup>Canada Research Chair in geochemistry of coastal hydrogeosystems, Québec-Océan, UQAR/ISMER, Rimouski,  
15 G5L 3A1, Canada

16 <sup>6</sup>Département de Géographie, Université Laval, Quebec City, G1V 0A6, Canada

17 <sup>7</sup>Institute of Geographic Sciences and Natural Resources Research, Chinese Academy of Science, Beijing, 100101,  
18 China

19 *Correspondence to:* Feng Wang (feng.wang@uqar.ca)

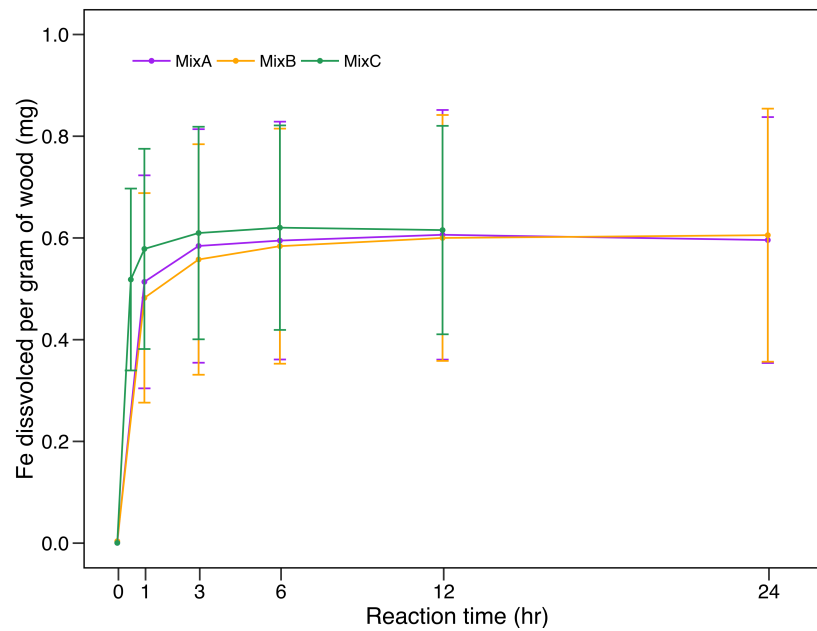


20

21

22

**Figure S1.** A general view of the staining issue of wet LSTs at the site L105. Note the blue-gray colors of many cross-sections sampled on lake subfossils.



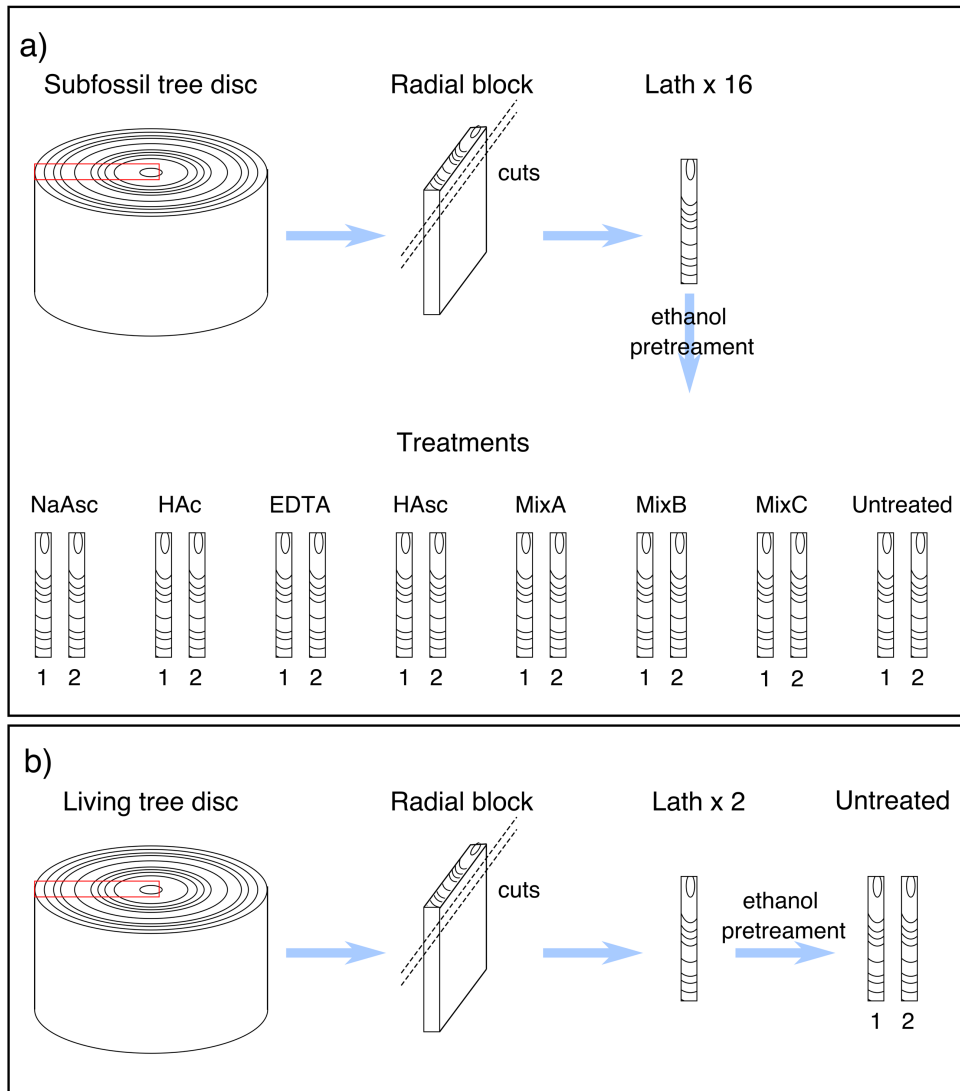
23

24

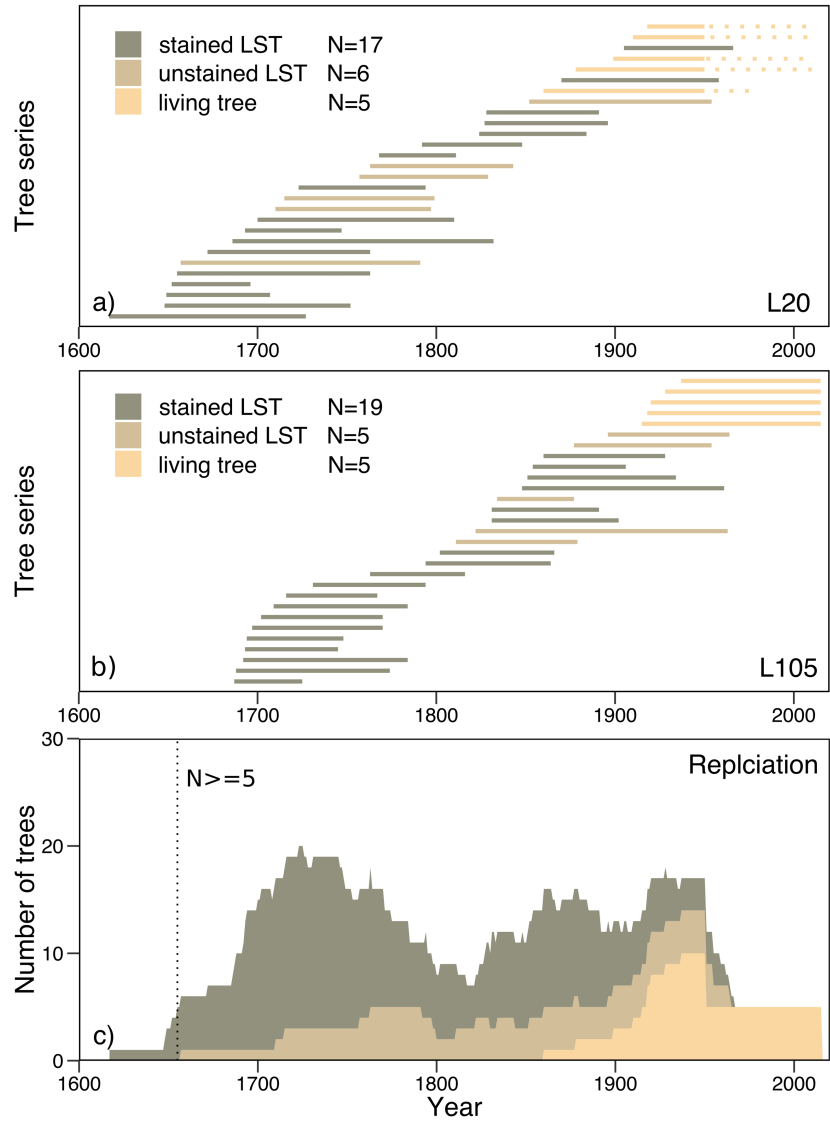
25

26

**Figure S2.** Fe dissolution curves during the MixA, MixB and MixC treatments. Dots and error bars refer to the mean and standard deviation values, respectively. Note that the reaction curve of MixC was computed from data of 9 LST replicates (10 for MixA and MixB).



27  
 28 **Figure S3.** Design of de-staining experiments following Section 2.2 showing how a subfossil tree replicate (a) and a  
 29 living-tree replicate (b) were cut into 1mm-thick laths and how these laths were treated using different chemical  
 30 reagents. Lath 1 and 2 of each pair were used to analyze the residual Fe and wood RGB intensities, respectively. In  
 31 total, ten subfossil tree replicates and ten living-tree replicates were processed following the corresponding  
 32 procedure.



33

34

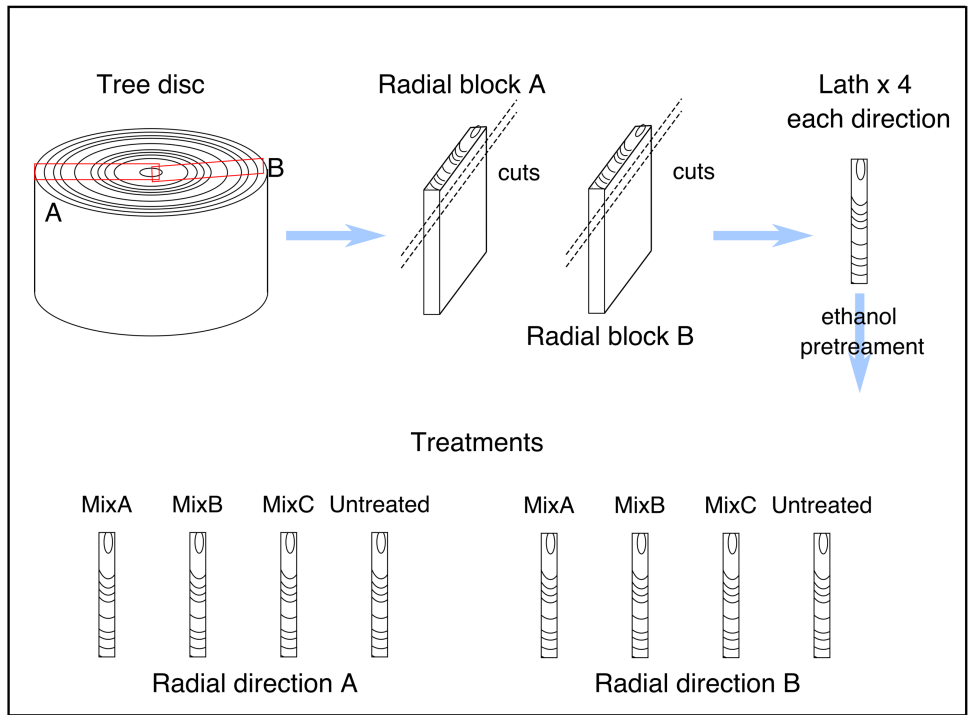
35

36

37

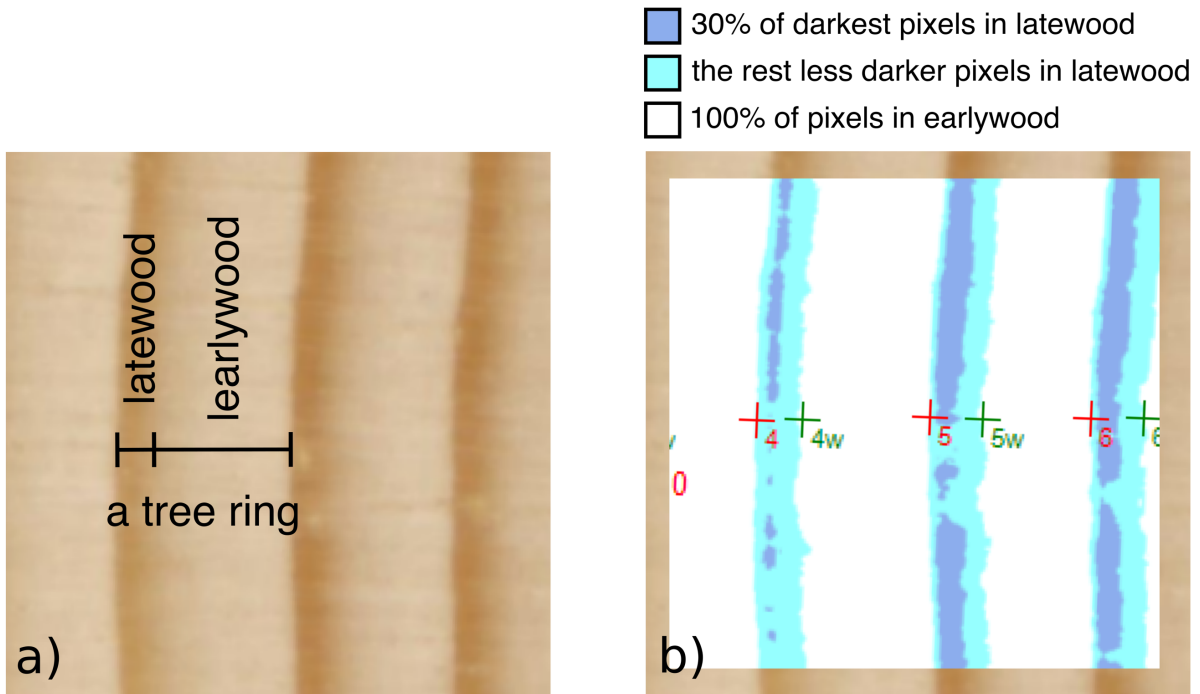
38

**Figure S4.** Timespans of tree-ring series used for developing LBI, DBI and MXD chronologies (a–b), and tree replication of the regional chronology (c). Dotted lines in (a) denote the post-1950 period at L20, for which living tree data were excluded due to the likely sapwood-heartwood color differences and unhealthy growth of trees. Note that LBI, DBI and MXD series share the same timespans and chronologies share the same tree replication because we kept only tree rings with measured values for all the three parameters (i.e. LBI, DBI and MXD).



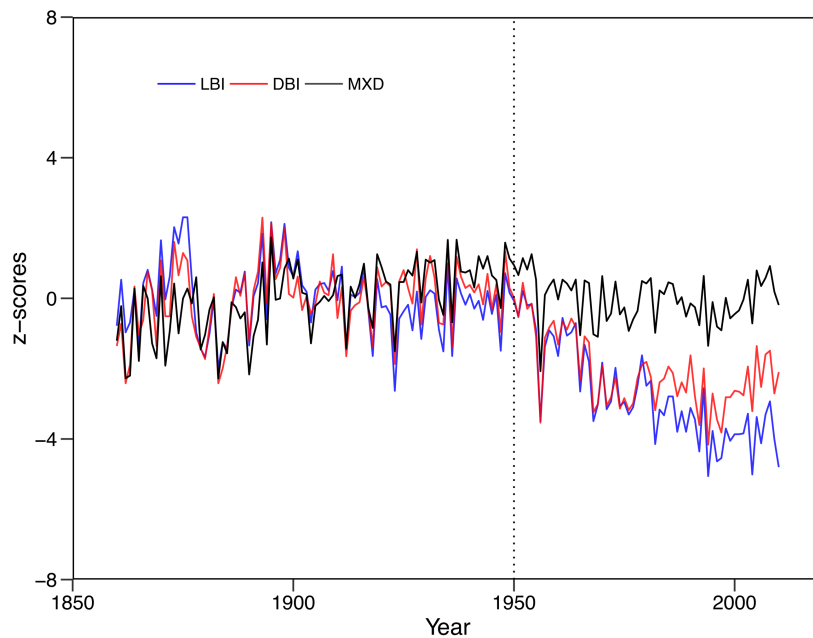
39  
40  
41  
42  
43

**Figure S5.** De-staining treatments of selected samples used for dendrochronological assessments following Section 2.3 showing how a tree replicate was cut into 1mm-thick laths and how these laths were treated using different chemical reagents. LBI, DBI and MXD series were measured from each lath after treatments. In total, 57 tree samples from L20 and L105 were processed following this procedure.



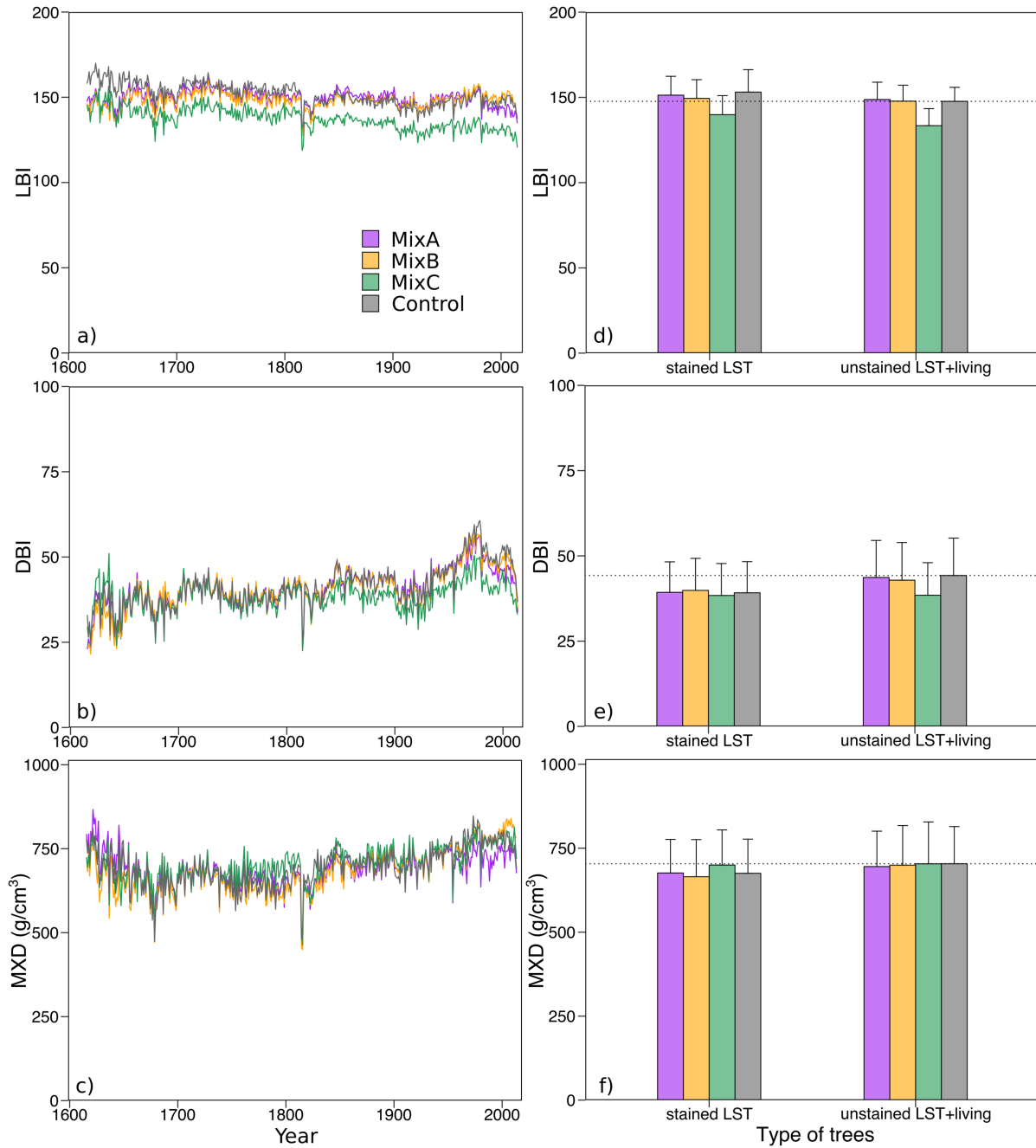
44  
45  
46  
47

**Figure S6.** Tree-ring structure (a) and an example of tree-ring color intensity measurement using Coorecorder 8.1 (Cybis Dendrochronology) (b).



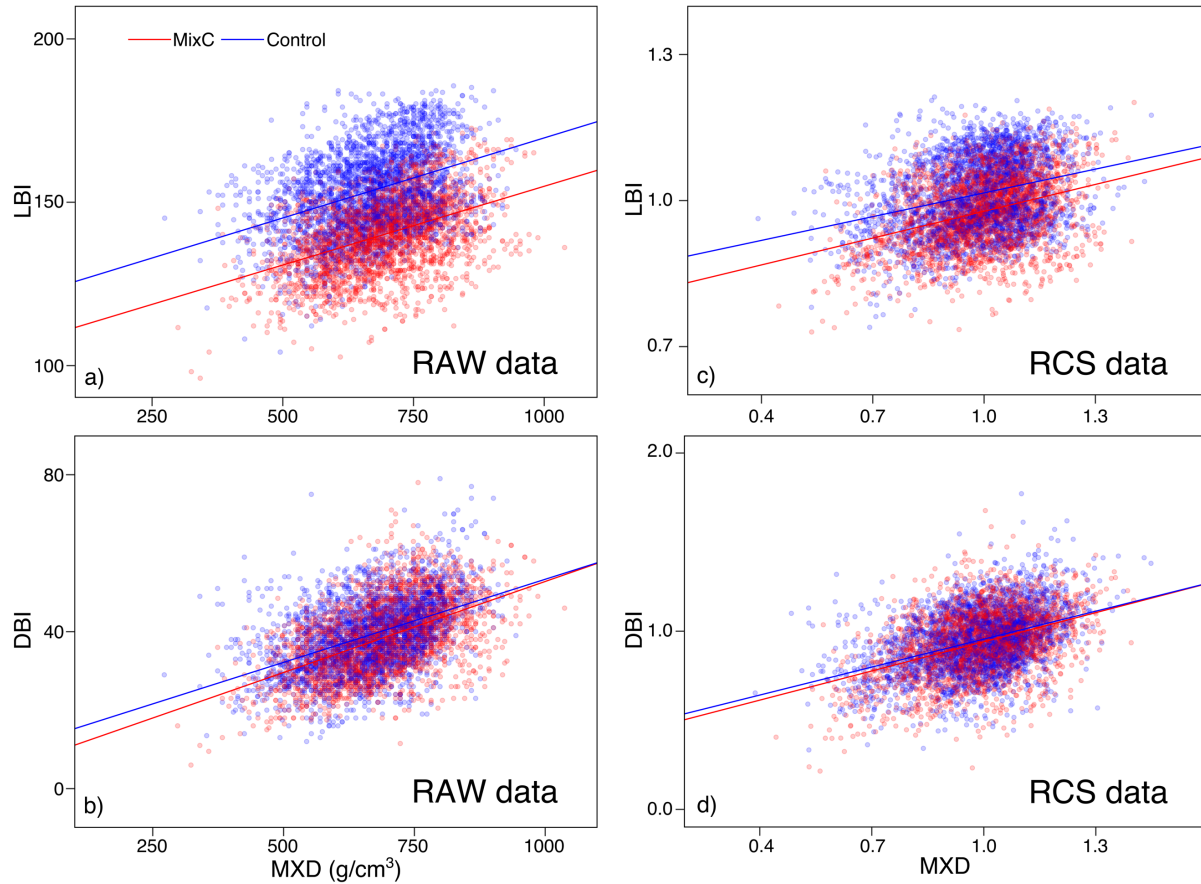
48  
49  
50  
51

**Figure S7.** Averaged raw measurements of LBI, DBI and MXD from five living trees at L20 (untreated with de-staining chemicals). Data are transformed to z-scores relative to the 1860–1950 time period. Dotted vertical line denotes the onset (1950) of BI divergence relative to MXD data.



52

53 **Figure S8.** Raw data of LBI, DBI and MXD of treated (MixA, MixB, MixC) and untreated (Control) LSTs and  
 54 living trees. (a)–(c) show the averaged mean value of the series according to calendar years. (d)–(f) show the  
 55 averaged data (bars) of stained LSTs and unstained LSTs+living trees, along with their standard deviations (error  
 56 bars). Dotted horizontal lines denote the averaged data of untreated, unstained LSTs+living trees.



57

58 **Figure S9.** Comparisons of LBI (a, c) and DBI (b, d) against MXD data for the MixC treated and Control stained  
 59 LSTs. Comparisons are based on raw data (left panel) and RCS standardized data (right panel). Straight lines are  
 60 linear regressions between BI and MXD data.

61

62 **Table S1.** Statistics of calibration (1901–1960) and verification (1960–2015) for LBI, DBI and MXD against the  
 63 May–August temperature target. All statistics in the table are significant  $p < 0.05$ , RE and CE > 0.

|                    | LBI vs Temp | DBI vs Temp | MXD vs Temp |
|--------------------|-------------|-------------|-------------|
| Full $r^2$         | 0.431       | 0.358       | 0.528       |
| Calibration $r^2$  | 0.427       | 0.429       | 0.464       |
| Verification $r^2$ | 0.246       | 0.088       | 0.443       |
| Verification RE    | 0.529       | 0.425       | 0.632       |
| Verification CE    | 0.216       | 0.043       | 0.388       |
| RMSE               | 0.112       | 0.096       | 0.144       |

64